Laurentthomasite, $Mg_2K(Be_2Al)Si_{12}O_{30}$: a new milarite-group-type member from the Ihorombe region, Fianarantsoa Province, Madagascar

Cristiano Ferraris[1], **Isabella Pignatelli**[2], **Fernando Cámara**[3], **Giancarlo Parodi**[1], **Sylvain Pont**[1], **Martin Schreyer**[4], **and Fengxia Wei**[5]

[1]Institut de Minéralogie, de Physique des Matériaux et de Cosmochimie, UMR 7590,
Muséum National d'Histoire Naturelle, CP 52, 61 rue Buffon, 75005 Paris, France
[2]Laboratoire GeoRessources, Université de Lorraine, Faculté des Sciences et Technologies, Rue Jacques Callot,
BP 70239, 54506 Vandœuvre-lès-Nancy, France
[3]Dipartimento di Scienze della Terra "A. Desio", Università degli Studi di Milano,
Via Mangiagalli, 34 – 20133 Milan, Italy
[4]Malvern Panalytical B.V., Lelyweg 1 (7602 EA), P.O. Box 13, 7600 AA Almelo, the Netherlands
[5]Institute of Materials Research and Engineering (IMRE),
2 Fusionopolis Way, Innovis, #08-03, 138634 Singapore

Correspondence: Cristiano Ferraris (ferraris@mnhn.fr)

Abstract. Laurentthomasite, ideally $Mg_2K(Be_2Al)Si_{12}O_{30}$, is a new milarite-group member found within quartz-syenite pegmatites from the Ihorombe region, Fianarantsoa Province, Madagascar. It occurs as euhedral {0001} hexagonal crystals, maximum 15 mm large and 5 mm thick. The crystals show a very strong dichroism with cobalt blue and green-yellow colours when observed along [0001] and [1000], respectively. The mineral is transparent, uniaxial (+) and its lustre is vitreous. The hardness is about 6 (Mohs scale), showing a poor {0001} cleavage, irregular to conchoidal fracture, and a measured density of $2.67(8)\,\text{g cm}^{-3}$. Laurentthomasite is hexagonal, space group $P6/mcc$ (no. 192), with $a = 9.95343(6)$ Å, $c = 14.15583(8)$ Å, $V = 1214.54(1)$ Å^3 and $Z = 2$. The strongest nine lines in the X-ray powder diffraction pattern [d in Å – (I) – hkl] are $3.171 – (10) – 211$, $4.064 – (8) – 112$, $2.732 – (8) – 204$, $4.965 – (6) – 110$, $2.732 – (4) – 204$, $3.533 – (3) – 004$, $7.055 – (2) – 002$, $4.302 – (2) – 200$ and $3.675 – (2) – 202$. Chemical analyses by electron microprobe and several spectroscopies (inductively coupled plasma, ICP; optical emission, OES; mass, MS; and Mössbauer) give the following empirical formula based on 30 anions per formula unit: $(Mg_{0.86}\,Sc_{0.54}\,Fe^{2+}_{0.35}\,Mn_{0.26})_{\sum=2.01}(K_{0.89}\,Na_{0.05}\,Y_{0.02}\,Ca_{0.01}\,Ba_{0.01})_{\sum=0.98}[(Be_{2.35}\,Al_{0.50}\,Mg_{0.11}\,Fe^{3+}_{0.03})_{\sum=2.99}(Si_{11.90}\,Al_{0.10})O_{30}]$; the simplified formula is $(Mg, Sc)_2(K, Na)[(Be, Al, Mg)_3(Si, Al)_{12}O_{30}]$. The crystal structure was refined to an R index of 1.89 % based on 430 reflections with $Io > 2\sigma(I)$ collected on a four-circle diffractometer with $CuK\alpha$ radiation. By comparison with the general formula of the milarite group, $A_2B_2C[T(2)_3T(1)_{12}O_{30}](H_2O)\,x$ ($0 < x < n$, with $n < 2$ pfu, per formula unit), the laurentthomasite structure consists of a beryllo-alumino-silicate framework in which the $T(1)$ site is occupied by Si and minor Al and forms $[Si_{12}O_{30}]$ cages linked by the $T(2)$ site mainly occupied by (Be + Al). The A and C sites occur in the interstices of the framework while the B site is vacant. The origin of the strong dichroism is related to a charge transfer process between Fe^{2+} and Fe^{3+} in octahedral A sites and tetrahedral $T(2)$ sites, respectively.

1   Introduction

Besides economic reasons, Madagascar's pegmatites are amongst the best research fields for mineral collectors because of both the size and the aesthetic characteristics of many different mineral species. Although there are more than 370 valid mineral species from approximately 1000 different localities in Madagascar (Mindat, 2020a), including a relatively large number of new mineral species containing the light elements Li, Be or B (Table 1), no new species belonging to the milarite group have been described. Milarite and osumilite have been reported in the central and southern regions of Amoron'i Mania and Anosy (Pezzotta, 2005; Holder et al., 2018), but laurentthomasite, $Mg_2K(Be_2Al)Si_{12}O_{30}$, is the first mineral species belonging to the milarite group for which Madagascar is the type locality.

Laurentthomasite $Mg_2K(Be_2Al)Si_{12}O_{30}$ is the anhydrous Mg-dominant analogue of milarite $Ca_2K(Be_2Al)Si_{12}O_{30}$ and was approved as a new mineral species in April 2019 by the Commission on New Minerals, Nomenclature and Classification (CNMNC) of the International Mineralogical Association (IMA) (2018–157) as a member of the milarite group (9.CM.05 in the classification of Strunz and Nickel, 2001).

The general formula of minerals belonging to the milarite group (Forbes et al., 1972) is $^{VI}A_2^{IX}B_2^{XII}C[^{IV}T(2)_3^{IV}T(1)_{12}O_{30}](H_2O)x$ with $x = 0 - n$ ($n < 2$ pfu – Gagné and Hawthorne, 2016a), with the following known site occupancies: $A = $ Al, Fe^{3+}, Sn^{4+}, Mg, Zr, Fe^{2+}, Ca, Na, Y or Sc; $B = $, Na, K or H_2O; $C = $, Na, K or Ba; $T(1) = $ Al or Si; and $T(2) = $ Li, Be, B, Mg, Al, Si, Mn, Fe^{2+} or Zn. Milarite-group minerals are double-ring silicates having maximum topological symmetry corresponding to space group $P6/mcc$, although cation ordering may lead to lower symmetry.

Together with the recent description of aluminosugilite (Nagashima et al., 2020), laurentthomasite attests to, once more, the great compositional flexibility of the milarite structure type; at the present time 25 members belong to this group, with the number constantly increasing from 15 in 1991 (Hawthorne et al., 1991) up to 23 in 2016 (Gagné and Hawthorne, 2016a).

Laurentthomasite captured our attention whilst analysing a set of gemstones coming from the south of Madagascar. Its dichroism going from deep blue to green yellow together with prismatic hexagonal crystals was a source of perplexity for collectors, since it could be confused with both corundum sapphire and/or cordierite, mineral species much more common in the Madagascan southern provinces. Both sapphire and cordierite were rejected based on hardness measurements: 6 vs. 7.5 and 9 (Mohs scale), respectively. On the other hand, the first results of chemical investigations showing the presence of elements such as Sc, K and Be stimulated our interest. Scandium-rich minerals are very rare: only 15 terrestrial mineral species have scandium as an important

constituent, while another five are of extraterrestrial origin (Mindat, 2020b)

The name laurentthomasite honours Laurent Thomas, born 1971 in Tours (Centre-Val de Loire, France). He has been a very active geologist, prospector and mineral dealer since the early 1990s, especially for African areas such as Madagascar. He is the one who first brought to the public knowledge some new species from Madagascar such as pezzottaite from Mandrosonoro, as well as new localities such those of grandidierite from Tranomaro, euclase from Itasy and chrysoberyl from Tsitondroina (see Lefevre and Thomas, 1998; Forner et al., 2001). The new mineral species and its name were approved by the Commission on New Minerals, Nomenclature and Classification, International Mineralogical Association (IMA 2018–157).

The laurentthomasite description is based on one holotype and two cotype specimens, which are deposited in the collections of the Muséum National d'Histoire Naturelle (MNHN) of Paris (France); catalogue numbers are MNHN_MIN_218.1_a for the holotype and MNHN_MIN_218.1_b and MNHN_MIN_218.1_c for cotypes.
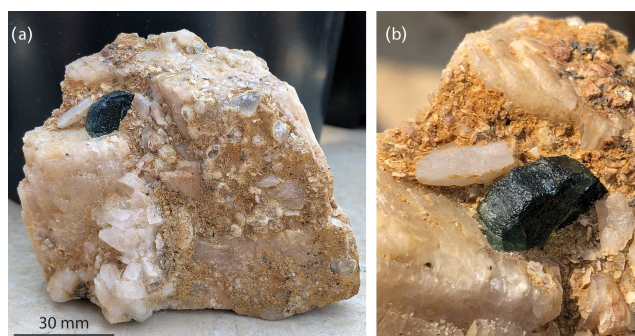
2   Geological settings

The studied samples were collected by Laurent Thomas in the Ihorombe region (Fianarantsoa Province) at about 80 km north-east of the village of Betroka (23°16′03″ S, 46°05′49″ E), in southern Madagascar. The area is located in the north-eastern part of the Ranotsara shear zone in the Antananarivo block, one of the five tectonic units into which Madagascar is divided (Collins et al., 2000; Collins and Windley, 2002). The Antananarivo block consists of 2550–2500 Myr granitoids tectonically interlayered with granites, syenites and gabbros (Tucker et al., 1999; Kröner et al., 2000). The whole of the Antananarivo block was thermally and structurally reworked between $\sim$ 750 and 500 Myr (Collins and Windley, 2002), with pre-existing rocks being metamorphosed to granulite facies and with the development of gneissic fabrics. Magmatism at circa 550 Myr produced granitoids bodies metres to kilometres across that are characteristic of this tectonic unit. Laurentthomasite was found within a pegmatite (coeval with these granitoid bodies) in a series of biotite- and amphibole-rich gneisses as well as migmatites and a set of pyroxene-rich alkali syenites (Besairie, 1959; Tucker et al., 1999; Kröner et al., 2000).

Laurentthomasite is associated with orthoclase, massive quartz, rare pale green apatite crystals, phenakite, beryl, albite, magnetite, thortveitite and cheralite (Fig. 1): at the microscopic scale unknown phases (currently under investigation) containing different ratios of Nb, Ta and W are also present. Due to the extremely weathered conditions of the few outcrops, pegmatite samples containing laurentthomasite are rare and deeply weathered into laterite; so far only

Table 1. Approved mineral species containing Li, Be and/or B from Madagascar.

Mineral	Formula	Reference*
Béhierite	$(Ta^{5+}, Nb^{5+})(BO_4)$	Fleischer (1962)
Bityite	$LiCaAl_2(AlBeSi_2O_{10})(OH)_2$	Lacroix (1908)
Fluor-liddicoatite	$Ca(Li_2Al)Al_6(Si_6O_{18})(BO_3)_3(OH)_3F$	Dunn et al. (1977)
Grandidierite	$(Mg,Fe^{2+})(Al,Fe^{3+})_3(SiO_4)(BO_3)O_2$	Lacroix (1902)
Laurentthomasite	$Mg_2K(Be_2Al)Si_{12}O_3$	This study
Londonite	$(Cs,K,Rb)Al_4Be_4(B, Be)_{12}O_{28}$	Simmons et al. (2001)
Manandonite	$Li_2Al_4(Si_2AlB)O_{10}(OH)_8$	Lacroix (1912)
Pezzottaite	$Cs(Be_2Li)Al_2(Si_6O_{18})$	Laurs et al. (2003)
Schiavinatoite	$(Nb,Ta)(BO_4)$	Demartin et al. (2001)
Vránaite	$Al_{16}B_4Si_4O_{38}$	Cempírek et al. (2016)

* References are those of the "The New IMA List of Minerals" updated to March 2020, available on the website (http://cnmnc.main.jp/, last access: 6 May 2020) of the Commission on New Minerals, Nomenclature and Classification (CNMNC) of the International Mineralogical Association (IMA).
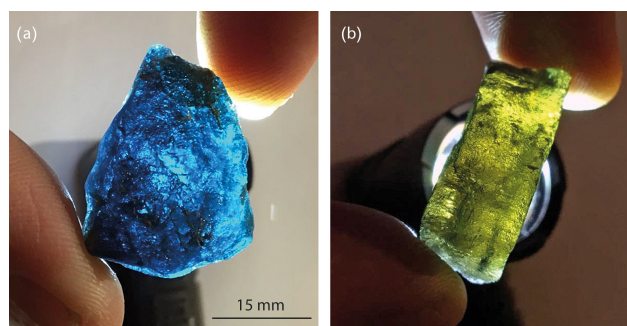

Figure 1. (a) Blue hexagonal crystal of laurentthomasite in partially weathered pegmatite mainly composed of quartz, orthoclase, phenakite and secondary apatite. **(b)** Enlargement of **(a)**.

Figure 2. Images showing the strong dichroism of laurentthomasite crystals. Under white light, crystals are deep cobalt blue along [0001] and yellow-green perpendicular to [0001].

one crystal in a matrix has been found, whilst isolated specimens are more common.

The genesis of the new mineral laurentthomasite is related to crystallization of Sc-enriched pegmatites like those occurring at the Tørdal pegmatite field in southern Norway (Steffenssen et al., 2019). In contrast to the Tørdal bodies, the Madagascan pegmatite where laurentthomasite was found does not have any garnet that could be a major host for scandium.
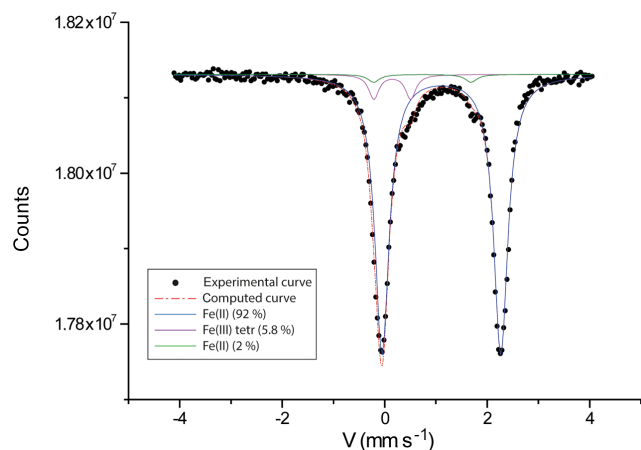
3 Appearance and physical properties

The sample material consists of tabular euhedral {0001} hexagonal crystals with maximum width and thickness values of 15 and 5 mm, respectively (Fig. 1a–b); all observed laurentthomasite crystals are characterized by dark micrometric inclusions of elongated crystals of an Fe^{2+}-rich phase as confirmed by Mössbauer spectroscopy. Observed forms are {1010} and {0001}. Crystals show a very strong dichroism with cobalt blue and green-yellow colours when observed along [0001] and [1000], respectively (Fig. 2a–b).

The origin of dichroism lies in the presence of the transition metal ions Fe^{2+} and Fe^{3+}, located in octahedral A sites and tetrahedral $T(2)$ sites, respectively, and inter-valence charge transfer between them. Twinning was not observed. The mineral has a light blue streak and is transparent and non-fluorescent. Its lustre is vitreous. The hardness is about 6 (Mohs scale) based on scratching tests, with poor cleavage parallel to {0001}. The tenacity is brittle with irregular to conchoidal fracture. Laurentthomasite has a measured density of 2.67(8) g cm⁻³ (hydrostatic balance) and a calculated density of 2.66(4) g cm⁻³ using the empirical formula.

In our 23 μm thick thin section, the mineral is colourless and pleochroism is not visible; it is optically uniaxial (+), with $\omega = 1.540(2)$ and $\varepsilon = 1.545(3)$ ($\lambda = 589$ nm) measured by refractometry; and dispersion was not observed. The compatibility index $(1 - K_P/K_C) = 0.028$ is rated as excellent (Mandarino, 1981).
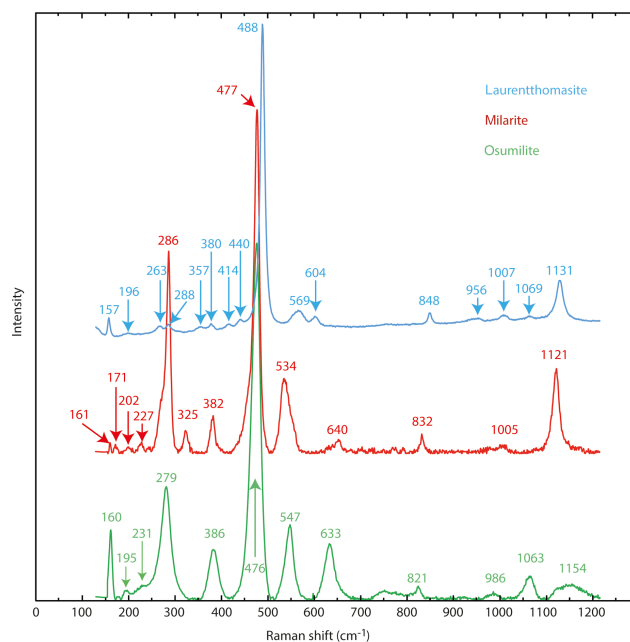
Figure 3. Deconvoluted Mössbauer spectrum of laurentthomasite.

4　Analytical methods

For elements heavier than carbon, wavelength-dispersive X-ray spectroscopy (WDS) 40-point analyses were performed with an electron microprobe CAMECA SX100 (Service d'Analyse Microsonde Camparis – Université Pierre et Marie Curie, Paris), at an accelerating voltage of 15 kV, a probe current of 10 nÅ and a beam diameter of 5 μm. Analysed elements and standards were Si, Mg and Ca (diopside); Al and K (orthoclase); Sc (synthetic Sc_2O_3); Ti and Mn (pyrophanite); Fe (hematite); Zn (sphalerite); Ba (baryte); and Na (albite). The polished section of the analysed crystal was free of inclusions, at least to the depth reached by the electron beam. Both beryllium and trace elements (including rare earth elements, REEs) were analysed using about 0.1 g of powdered sample by inductively coupled plasma optical emission spectrometry (ICP-OES) and mass spectrometry (ICP-MS) at the SARM laboratory of CRPG-CNRS. The amount of Fe^{3+} within the structure was deduced from Mössbauer spectroscopy (Fig. 3). The miniaturized Mössbauer spectrometer (MIMOS II) developed by Klingelhöfer et al. (1996) at the LCPME laboratory (Université de Lorraine, France) was used to investigate the oxidation state of iron in laurentthomasite samples.

Raman spectra (Fig. 4) were obtained using a modified Princeton Instruments spectrometer at the IMPMC (Institut de minéralogie, de physique des matériaux et de cosmochimie, Université Pierre et Marie Curie, Paris, France). The instrument is synchronized with a nanosecond pulsed diode pumped solid state (DPSS) laser operating at 532 nm with a 1.5 ns duration for the pulse, a 10 to 2000 Hz repetition rate and up to 1 mJ output energy per pulse. The spectrometer was synchronized and optimized to collect the signal only during the laser pulse in order to minimize the luminescence background.

Figure 4. Raman spectrum of laurentthomasite compared to those of milarite and osumilite.

Powder diffraction X-ray data were collected between 4 and 100° ($CuK\alpha$1-2-circle θ-θ goniometer) using a Bragg-Brentano X'pert Pro MPD diffractometer at the IMPMC.

A single-crystal (39.6 μm × 28.7 μm × 16.9 μm) was analysed using an X-ray diffraction four-circle Agilent Super-Nova instrument at the Institute of Materials Research and Engineering of Singapore ($CuK\alpha$ radiation); the data were collected in the 2θ range 0.279 to 113.785° at 10 s exposure for each frame (0.029° width) and integrated by the software CrysAlis^{Pro}; empirical absorption correction was applied.

5　Results

5.1　Chemical analyses

Tables 2 and 3 show the chemical composition of laurentthomasite. The deconvoluted experimental Mössbauer spectrum shows the presence of two types of octahedral Fe^{2+}: the blue and the green curves belong to the laurentthomasite and the inclusions mentioned above, respectively (Fig. 3). As shown in Table 4 the Fe^{2+} and Fe^{3+} relative contents of laurentthomasite are 92.0 % and 5.8 %, respectively. Thus, after normalizing to 100 %, Fe^{2+} constitutes 94 % of the Fe in laurentthomasite itself. The violet doublet represents the tetrahedral Fe^{3+} contained within laurentthomasite; the centre shifts (CS), quadrupole splitting (QS) and relative areas are reported in Table 4.

In Fig. 4 the Raman spectrum of laurentthomasite is compared to those of milarite and osumilite (Lafuente et al., 2015). The spectra are very similar in having the most intense

Table 2. WDS and ICP-OES-MS chemical analyses of laurentthomasite.

Constituent	Wt. %	Range	SD	Probe standard
SiO_2	73.10	71.29–74.90	0.41	Diopside
Al_2O_3	3.11	3.03–3.20	0.05	Orthoclase
Sc_2O_3	3.78	3.70–3.86	0.05	Synthetic Sc_2O_3
Y_2O_3*	0.22			
TiO_2	0.02	0.02–0.019	0.01	Pyrophanite
FeO	2.69	2.50–2.67	0.07	Hematite
Fe_2O_3**	0.19			
MnO	1.91	1.77–2.04	0.07	Pyrophanite
MgO	4.01	3.80–4.09	0.07	Diopside
ZnO	0.04	0.01–0.07	0.03	Sphalerite
CaO	0.07	0.06–0.08	0.01	Diopside
BaO	0.16	0.09–0.23	0.04	baryte
BeO*	6.02			
Na_2O	0.15	0.10–0.18	0.02	albite
K_2O	4.30	3.92–4.67	0.03	orthoclase
Total	99.77			

* Measured by ICP-MS; the analytical uncertainty for both Y and Be contents is < 5 %. ** The amount of Fe_2O_3 was calculated starting from analysed FeO and the results of Mössbauer spectroscopy.

Table 3. Trace element contents of laurentthomasite.

Elem.	$\mu g\,g^{-1}$	Uncertainty
As	36.6	< 10 %
Bi	0.07	< 20 %
Cd	0.07	< 20 %
Co	3.49	< 20 %
Cr	5.5	< 10 %
Cs	82.9	< 5 %
Cu	3.0	< 20 %
Ga	37.3	< 10 %
Ge	2.15	< 10 %
Hf	6.59	< 10 %
In	7.72	< 15 %
Mo	n.d*.	< D.L.**
Nb	2.99	< 10 %
Ni	15.3	< 5 %
Pb	0.85	< 20 %
Rb	1405	< 1 %
Sb	0.57	< 20 %
Sn	2.36	< 20 %
Sr	21.2	< 15 %
Ta	2.02	< 10 %
Th	0.87	< 20 %
U	0.70	< 20 %
V	3.4	< 15 %
W	n.d*	< D.L.**
Y	1754	< 1 %
Zn	176	< 5 %
Zr	7.81	< 15 %
La	1.50	< 20 %
Ce	3.62	< 15 %
Pr	0.749	< 20 %
Nd	3.88	< 15 %
Sm	3.07	< 10 %
Eu	0.239	< 15 %
Gd	5.56	< 10 %
Tb	2.32	< 15 %
Dy	29.4	< 10 %
Ho	12.8	< 10 %
Er	91.2	< 5 %
Tm	43.4	< 5 %
Yb	922	< 1 %
Lu	321	< 1 %

* n.d: not detected. * D.L.: detection limit.

peak around $480\,cm^{-1}$ and comparable to the known spectra of other milarite-group minerals like brannockite, chayesite, or poudretteite (Lafuente et al., 2015) or friedrichbeckeite, and almarudite (Lengauer et al., 2009). Differences in Raman shifts of individual bands are due to the chemical variations, bond geometries and bond strengths for different mineral species. Figure 4 clearly shows that the laurentthomasite spectrum shares more affinities with the osumilite than with milarite; the most pronounced difference between the three spectra is the splitting of bands around $280\,cm^{-1}$, with an evident separation into two components with maxima at 263 and $288\,cm^{-1}$ for laurentthomasite.

The empirical formula based on 30 anions pfu (per formula unit) is $(Mg_{0.86}\ Sc_{0.54}\ Fe^{2+}_{0.35}\ Mn_{0.26})_{\sum=2.01}\ (K_{0.89}\ Na_{0.05}\ Y_{0.02}\ Ca_{0.01}\ Ba_{0.01})_{\sum=0.98}\ [(Be_{2.35}\ Al_{0.50}\ Mg_{0.11}\ Fe^{3+}_{0.03})_{\sum=2.99}\ (Si_{11.90}\ Al_{0.10})\ O_{30}]$. The simplified formula is $(Mg, Sc)_2(K, Na)[(Be, Al, Mg)_3(Si, Al)_{12}O_{30}]$, while the ideal formula is $Mg_2K(Be_2\ Al)Si_{12}O_{30}$, requiring K_2O 4.96, BeO 5.27, MgO 8.49, Al_2O_3 5.37 and SiO_2 75.92 for a total of 100 wt. %.

5.2 Crystallographic data

The cell parameters obtained from Rietveld refinement of the X-ray powder diffraction data (HighScore suite program, Degen et al., 2014) (Fig. 5; Table 5) are $a = 9.95343(6)$ Å, $c = 14.15583(8)$ Å, $V = 1214.54(1)$ Å^3 and $Z = 2$. Parameters used for the Rietveld refinement were (a) the 0 shift fixed at 0, (b) the background modelled using a flat and a $1/X$ background as well as five parameters of a Chebyshev function, (c) isotropic displacement parameters for each atomic positions, (d) atomic occupancies for the non-oxygen positions, (e) the peak shape modelled using a pseudo-Voigt func-
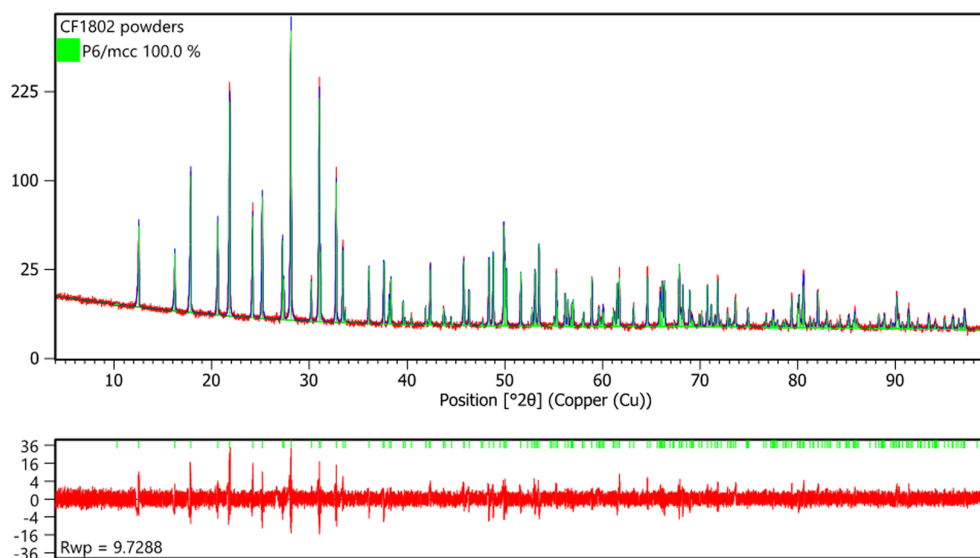
tion with Finger–Cox–Jephcoat (FCJ) asymmetry (Finger et al., 1994) rather than a fundamental parameter approach so the microstructural parameters like size and strain were not refined, and (f) the preferred orientation was not refined.

Single crystal X-ray diffraction investigations show that laurentthomasite belongs to the hexagonal crystal system with space group $P6/mcc$ (no. 192) and unit cell parameters $a = 9.95800(7)$ Å, $c = 14.114916(11)$ Å, $V = 1215.081(15)$ Å^3 and $Z = 2$ (Table 6). The structure of laurentthomasite was refined using SHELXL-2012 (Sheldrick,

Figure 5. Rietveld refinement of the X-ray powder diffraction pattern of laurentthomasite.

Table 4. Parameters from fitting of the Mössbauer spectrum.

Element	CS (mm s^{-1})	QS (mm s^{-1})	RA (%)
Fe(II) octa$_{Laur}$	1.21	2.31	92.0
Fe(III) tetra$_{Laur}$	0.25	0.71	5.8
Fe(II) octa$_{Incl}$	0.85	1.9	2.2

Incl: inclusions. Laur: laurentthomasite. CS: centre shift. QS: quadrupole splitting. RA: relative areas.

2015) starting from the atom coordinates of oftedalite (Cooper et al., 2006). Scattering curves of fully ionized species were used at cation sites (Rossi et al., 1983; Hawthorne et al., 1995): for the $T(1)$ site ionized Si was refined vs. neutral Si; according to information from chemical analyses and also the fact that Fe and Mn have very similar scattering factors, $Fe^{2+} + Mn^{2+}$ (0.61 apfu, atoms per formula unit) was constrained to be equal to Sc^{3+} (0.54 apfu) and then refined versus Mg^{2+} at the A site. Neutral vs. ionized scattering curves were used at oxygen sites (Rossi et al., 1983; Hawthorne et al., 1995). The Fourier difference map did not reveal any maximum above $0.29\,e^{-}\,Å^3$. Anisotropic full-matrix least-squares refinement on F_o^2 yielded $R_1 = 1.89\%$ [430 reflections with $I_o > 2\sigma I$] and $R_{all} = 1.89\%$ (431 reflections). Experimental details are reported in Table 6. Refined atom coordinates and equivalent isotropic displacement parameters are reported in Table 7. Selected interatomic distances and bond angles are given in Table 8. A Crystallographic Information File (CIF) and list of observed and calculated structure factors are available as electronic material. The structure is isotypic with minerals of the milarite group (Gagné and Hawthorne, 2016a).

6   Discussion

As discussed by Gagné and Hawthorne (2016a), the structure of the milarite-group minerals is a beryllo-alumino-silicate framework consisting of a four-connected three-dimensional net.

The majority of the minerals belonging to the milarite group can be described with space-group symmetry $P6/mcc$ (Gagné and Hawthorne, 2016a), which is reduced to $P62c$ and $Pnc2$ because of cation ordering in respectively roederite and armenite (Armbruster, 1989, 1999).

The main feature of the laurentthomasite structure is a $[T(1)_{12}O_{30}]$ unit consisting of double six-membered rings of corner-linked SiO_4 tetrahedra (Fig. 6). These rings are stacked along the c axis, thus establishing a channel system along [0001]. These units are interconnected by sharing corners with $T(2)O_4$ tetrahedra. These obtained structural blocks are arranged in groups of three around one centrally located AO_6 octahedron. The C site is situated in the centre of the channel between two $[T(1)_{12}O_{30}]$ units (Fig. 7).
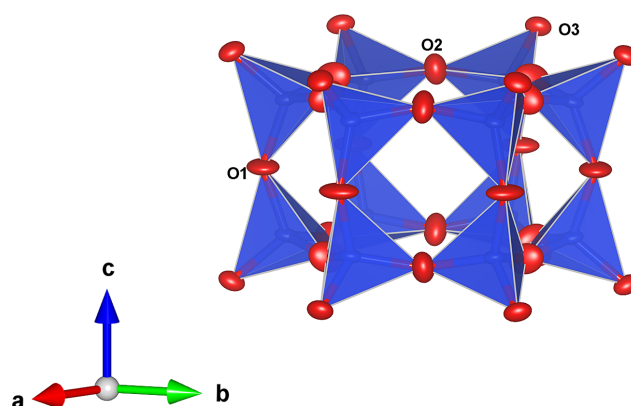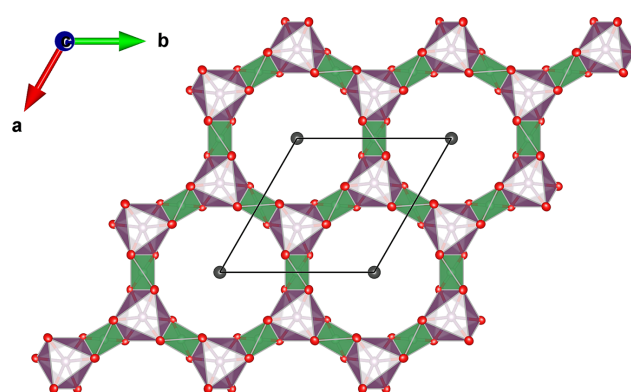
Laurentthomasite presents the charge arrangement [10] of Gagné and Hawthorne (2016b). It is related to oftedalite ($ScCaKBe_3Si_{12}O_{30}$; Cooper et al., 2006) by the $(^A Sc^{T(2)}Be)_{-1}(^A Mg^{T(2)}Al)$ and $^A Ca^A_{-1}Mg$ substitutions, to milarite ($Ca_2KBe_2AlSi_{12}O_{30}$) by the $^A Ca^A_{-2}Mg_2$ substitution, and to friedrichbeckeite ($Mg_2NaKBe_3Si_{12}O_{30}$; Lengauer et al., 2009) by the $(^B Na^{T(2)}Be)_{-1}(^B\square^{T(2)}Al)$ substitution.

Hawthorne et al. (1991) observed $<T\text{-}O>$ distances of 1.609–1.612 Å for several milarite crystals with $T(1) = (Si_{11.89}\text{-}Si_{12})$: mean value of 1.611 Å. Anyway, the observed $<T(1)\text{–}O>$ distance, $1.608(2)$ Å (Table 8), is compatible with the full occupancy of Si at the $T(1)$ site, and it compares well, within experimental error, with the distances observed

Table 5. X-ray powder diffraction data for laurentthomasite.

I	d-obs [Å]	d-calc [Å]	h	k	l
2	7.055	7.078	0	0	2
1	5.457	5.470	1	0	2
6	4.965	4.977	1	1	0
2	4.302	4.310	2	0	0
8	4.064	4.071	1	1	2
2	3.675	3.681	2	0	2
3	3.533	3.539	0	0	4
1	3.269	3.274	1	0	4
1	3.253	3.258	2	1	0
10	3.171	3.175	2	1	1
1	2.956	2.960	2	1	2
8	2.881	2.884	1	1	4
1	2.870	2.873	3	0	0
4	2.732	2.735	2	0	4
1	2.678	2.681	2	1	3
1	2.486	2.488	2	2	0
1	2.388	2.391	3	1	0
1	2.345	2.348	2	2	2
1	2.131	2.133	3	1	3
1	1.980	1.981	3	1	4
1	1.880	1.881	4	1	0
1	1.863	1.865	4	1	1
2	1.825	1.827	3	1	5
1	1.822	1.823	3	0	6
1	1.817	1.818	4	1	2
1	1.768	1.769	0	0	8
1	1.723	1.724	5	0	0
1	1.711	1.712	2	2	6
1	1.660	1.661	4	1	4
1	1.566	1.567	4	1	5
1	1.506	1.507	3	0	8
1	1.501	1.502	3	3	4
1	1.441	1.442	2	2	8
1	1.411	1.412	4	2	5
1	1.407	1.408	6	0	2
1	1.380	1.380	5	2	0
1	1.373	1.374	5	2	1
1	1.331	1.331	6	0	4
1	1.313	1.314	3	1	9
1	1.191	1.191	5	2	6
1	1.004	1.004	1	0	14

Figure 6. The double ring of $T(1)$ tetrahedra, obtained with VESTA 3.0 (Momma and Izumi, 2011).

Figure 7. The $A - T(2)$ layer forming 12 rings. These rings are aligned with six-membered double Si rings along [0001]. C sites are located at the centre of these channels. $T(2)$ sites are shown in green; A sites are shown in pink. Diagram obtained with VESTA 3.0 (Momma and Izumi, 2011).

in other $^{T(1)}$Si members of the milarite group, as for instance 1.609 Å in sugilite (Armbruster and Oberhänsli, 1988) or 1.610 Å in aluminosugilite (Nagashima et al., 2020). Therefore, even if the empirical formula of laurentthomasite shows Si = 11.90 apfu vs. Al = 0.10 apfu, the scattering curve of Al was not taken into account during refinement. The tetrahedral quadratic elongation value (TQE) (Table 8), as defined in Robinson et al. (1971), shows that the $T(1)$ site is rather regular (7.39°^{2}), whereas the $T(2)$ sites is much more distorted [see the tetrahedral angle variance (TAV = 196.13°^{2})], in agreement with a mixed occupancy site.

The observed $< T(2)–O >$ distance of 1.674(1) Å (Table 8) is slightly larger than the predicted value of 1.637 Å (Gagné and Hawthorne, 2016b) for a pure $^{[4]}$Be−O bond length. As, according to the chemical analysis, the $T(2)$ occupancy, besides the presence of Be^{2+} (2.35 apfu) and Al (0.50 apfu), also shows the presence of Mg (0.11 apfu) and a very small amount of Fe^{3+} determined by Mössbauer spectroscopy. Considering thus a $^{[4]}$Mg−O of 1.939 Å (Gagné and Hawthorne, 2016b), and the larger ionic radius of Al^{3+} with respect to Be^{2+}, one can easily justify the slightly higher value (1.674 vs. 1.637 Å). The refined occupancy for Be is 0.74(1) atoms per site (i.e. 2.22 apfu) (Table 7), which is comparable to the one resulting from chemical analyses (2.35 apfu), and the refined occupancy of Al (inclusive of Mg and Fe), at $T(2)$ of 0.26(1) (i.e. 0.78 apfu). The refined site scattering at $T(2)$ is therefore 18.82 epfu (electrons per formula unit), and compared to the scattering calculated from chemistry (18.0 epfu), this indicates that, in the crystal studied by single crystal X-ray diffraction, Mg^{2+} at $T(2)$

Table 6. Crystal data and structure refinement for laurentthomasite.

Temperature	296(2) K
Space group	$P6/mcc$
Crystal size (mm)	$0.40 \times 0.29 \times 0.17$
Unit cell dimensions	a (Å) $= 9.95800(10)$ Å
	c (Å) $= 14.14920(10)$ Å
	V (Å^3) $= 1215.085(19)$
$D_{calc.}$	2.66(4) g cm^{-3}
$D_{obs.}$	2.67(8) g cm^{-3}
Radiation	Cu $K\alpha$ (1.54184 Å)
Monochromator	mirror optics
Diffractometer	SuperNova, Dual, AtlasS2
Scan type	ω scan
Absorption correction	CrysAlis^{Pro} (Oxford Diffraction/Agilent
	Technologies UK Ltd, Yarnton, England)
μ (mm^{-1})	5.269
θ_{min} (°)	5.13
θ_{min} (°)	72.72
Reflections collected	13424
Independent reflections	431
R_{int} (%)	6.42
R_{sig} (%)	1.35
Index limits	$-12 \leq h \leq 12, -12 \leq k \leq 12, -17 \leq l \leq 17$
Completeness to $\theta = 72.72°$	100.0 %
Refinement on F^2 using	SHELXL-2012 (Sheldrick, 2015)
Data/restraints/parameters	431/0/50
Goodness of fit on F^2	1.224
R_1 (%)	1.89
wR_2 (%)	4.76
Extinction coefficient	0.0038(2)
$\Delta\rho_{max}$ (e Å^{-3})	0.300 at 0.78 Å from $T(1)$
$\Delta\rho_{min}$ (e Å^{-3})	-0.219 at 2.10 Å from C

Table 7. Atomic coordinates, chemical site occupancies (occ.), electrons per site and isotropic displacement parameters U^{eq} for laurentthomasite. Wyck. stands for Wyckoff positions.

Site	Wyck.	x	Y	z	occ.	s.s. XRD/EMP e.p.s.*	U^{eq}
C	$2a$	0	0	1/4	K$^+$ 1.005(8)	19.1(2)/19	0.0224(5)
A	$4c$	1/3	2/3	1/4	Sc^{3+} 0.285(4) + Fe^{2+}	18.56(8)/18.51	0.0113(3)
					0.285(4) + Mg^{2+} 0.430(9)		
$T(1)$	$24m$	0.09704(5)	0.35423(5)	0.10773(3)	Si^{4+} 0.27(5) + Si^0 0.73(5)	14/14	0.0065(2)
O1	$24m$	0.1146(2)	0.4129(2)	0	O$^=$ 0.66(8) + O^0 0.34(8)	8/8	0.0160(4)
O2	$12l$	0.20991(14)	0.28450(15)	0.12663(9)	O$^=$ 0.67(6) + O^0 0.33(6)	8/8	0.0163(3)
O3	$24m$	0.13114(13)	0.48954(13)	0.18109(8)	O$^=$ 0.92(5) + O^0 0.08(5)	8/8	0.0099(3)
$T(2)$	$6f$	0	1/2	1/4	Be^{2+} 0.745(7) + Al^{3+} 0.255(7)**	6.30(6)/5.88	0.0103(7)

* s.s. is site scattering, XRD is X-ray diffraction, EMP is electron microprobe and e.p.s. is electrons per site. ** The Al also accounts for Mg.

might be lower (or even $^{[4]}$Fe^{3+} higher up to 0.06 apfu). Better agreement could be obtained with only Al and Be at $T(2)$, although this is not supported by chemical analyses nor supported by the mean bond length at $T(2)$. Allocation of 0.03 apfu Fe^{3+} at this site seems to be in agreement with the larger size observed. On the basis of the assumed mixed occupancy of $T(2)$, the calculated value [using bond-distances

from Shannon, 1976 and Gagnè and Hawthorne, 2016a] is 1.665 Å, in reasonable agreement with the observed value of 1.674 Å.

The refinement yields a C site fully occupied by K (19.1 epfu), in good agreement with the chemical analysis that shows 0.89 K + 0.05 Na + 0.02 Y + 0.01 Ca + 0.01 Ba = 0.98 apfu,

Table 8. Bond lengths (Å) for laurentthomasite.

$T(1)$-O3	1.5971(9)	$T(2)$-O3 ×4	1.6742(11)
$T(1)$-O1	1.6103(6)	TQE	1.0538
$T(1)$-O2	1.6116(16)	TAV ($°^2$)	196.13
$T(1)$-O2	1.6130(15)		
$< T(1)$-O>	1.608	A–O3 ×6	2.1364(10)
TQE	1.0019	OQE	1.0521
TAV ($°^2$)	7.39	OAV ($°^2$)	166.92
		C-O2 ×12	3.0856(13)

OAV: octahedral angle variance; OQE: octahedral quadratic elongation;
TAV: tetrahedral angle variance; TQE: tetrahedral quadratic elongation, as
defined in Robinson et al. (1971).

corresponding to a calculated site scattering of 19.0 epfu. The $< C$–O$ >$ distance, 3.086(1) Å (Table 8), is in good agreement with the $^{[12]}$K–O bond length (3.095 Å) predicted by Gagné and Hawthorne (2016b) of 3.095 Å, considering the presence of about 10 % smaller cations (Na, Ca and Ba).

The A site is a strongly distorted octahedron as shown by the octahedral angle variance (OAV = 166.92°, Table 8); the observed $< A$–O$ >$ distance of 2.136(1) Å (Table 8) is slightly longer than predicted for a pure $^{[6]}$Mg–O bond length (2.089 Å) (Gagné and Hawthorne, 2016b). Considering the A site population obtained by chemical analyses ($\sum A^{2+} =$ 1.47 apfu) and taking into account the quite significant presence of Sc (0.54 apfu), one could justify the derived longer value, given the $^{[6]}$Sc–O bond length (2.121 Å: Cong et al., 2010; bixbyite-type Sc_2O_3). Nevertheless, the presence of 0.61 apfu of Fe^{2+} and Mn^{2+} (0.35 Fe^{2+}0.26 Mn) also contributes to the lengthening of the $< A$–O$ >$ mean bond distance, in closer agreement with the observed value. However, this is not yet enough because the calculated mean bond length is 2.123(1) Å (using the ionic radii of Shannon, 1976) (Table 8). The A site is therefore larger than expected; this is probably due to (i) the A octahedron sharing three edges with three $T(2)$ tetrahedra as well as to (ii) an increased charge at the $T(2)$ site due to some replacement of Be by Al (and minor Fe^{3+}). All these features induce an increase of the A–O(3) bond distance. Incidentally, the refined ionization of O3 shows almost completely ionized oxygen at that site (92 %), compared with ionization refined at O1 and O2 sites (ca. 65 %, Table 7). This should be ascribed to the strong incidence of charge at the O3 site, which is threefold coordinated with one $T(2)$ site, one $T(1)$ site and one A site, whereas the O1 site is twofold bonded just to two Si^{4+} at the $T(1)$ site, and the O2 site is threefold bonded to two Si^{4+} at the $T(1)$ site and has a long bond to K^+ at the C sites. It is therefore more plausible to have a more covalent bond at the O1 and O2 sites, in full agreement with refinement. The refined scattering (37.12 epfu – Table 7) of the A site is in very good agreement with the chemical analysis (37.2 epfu). The Fourier difference map clearly indicates that the B sites are vacant in laurentthomasite.

The milarite group has yet again demonstrated an extraordinary versatility in its crystal chemistry.

References

Armbruster, T.: Crystal chemistry of double-ring silicates: structure of roedderite at 100 and 300 K, Eur. J. Mineral, 1, 701–714, 1989.

Armbruster, T.: Si, Al ordering in the double-ring silicate armenite, $BaCa_2Al_6Si_9O_{30} \bullet 2H_2O$: A single-crystal X-ray and ^{29}Si MAS NMR study, Am. Mineral., 84, 92–101, 1999.

Armbruster, T. and Oberhänsli, R.: Crystal chemistry of double-ring silicates: Structures of sugilite and brannockite, Am. Mineral., 73, 595–600, 1988.

Besairie, H.: Rapport annuel du Service Géologique de la République Malgache, 303 pp., 1959.

Cempírek, J., Grew, E. S., Kampf, A. R., Ma, C., Novák, M., Gadas, P., Škoda, R., Vašinová-Galiová, M., Pezzotta, F., Groat, L. A., and Krivovichev, S.: Vránaite, ideally $Al_{16}B_4Si_4O_{38}$, a new mineral related to boralsilite, $Al_{16}B_6Si_2O_{37}$, from the Manjaka pegmatite, Sahatany Valley, Madagascar, Am. Mineral., 101, 2108–2117, https://doi.org/10.2138/am-2016-5686, 2016.

Collins, A. S. and Windley, B. F.: The tectonic evolution of central and northern Madagascar and its place in the final assembly of Gondwana, J. Geol., 110, 325–340, 2002.

Collins, A. S., Windley, B. F., and Razakamanana, T.: Neoprotero-zoic extensional detachment in central Madagascar: implications for the collapse of the East African Orogen, Geol. Mag., 137, 39–51, 2000.

Cong, H., Zhang, H., Yao, B., Yu, W., Zhao, X., Wang, J., and Zhang, G.: ScVO$_4$: Explorations of novel crystalline inorganic optical materials in rare-earth ortho-vanadate systems, Cryst. Growth Des., 10, 4389–4400, https://doi.org/10.1021/cg1004962, 2010.

Cooper, M. A., Hawthorne, F. C., Ball, N. A., Černý, P., and Kristiansen, R.: Oftedalite, $(Sc, Ca, Mn^{2+})_2K(Be, Al)_3Si_{12}O_{30}$, a new member of the milarite group from the Heftetjern pegmatite, Tørdal, Norway: description and crystal structure, Can. Miner., 44, 943–949, https://doi.org/10.2113/gscanmin.44.4.943, 2006.

Degen, T., Sadki, M., Bron, E., König, U., and Nénert, G.: The High Score Suite, J. Powder Diff., 29–2, 13–18, https://doi.org/10.1017/S0885715614000840, 2014.

Demartin, F., Diella, V., Gramaccioli, C. M., and Pezzotta, F.: Schiavinatoite, (Nb,Ta)BO$_4$, the Nb analogue of behierite, Eur. J. Mineral., 13, 159–165, https://doi.org/10.1127/0935-1221/01/0013-0159, 2001.

Dunn, P. J., Appleman, D. E., and Nelen, J. E.: Liddicoatite, a new calcium end-member of the tourmaline group, Am. Mineral., 62, 1121–1124, 1977.

Finger, L. W., Cox, D. F., and Jephcoat, A. P.: A correction for powder diffraction peak asymmetry due to axial divergence, J. Appl. Crystallogr., 27, 892–900, https://doi.org/10.1107/S0021889894004218, 1994.

Fleischer, M.: New Mineral Names, Am. Mineral., 414, 14–420, 1962.

Forbes, W. C., Baur, W. H., and Khan, A. A.: Crystal chemistry of milarite-type minerals, Am. Mineral., 57, 463–472, 1972.

Forner, H., Gautier, F., and Thomas, L.: Les macles de quartz de la région d'Andilamena, Madagascar, Le Règne Minéral, 39, 42–46, 2001.

Gagné, O. C. and Hawthorne, F. C.: Chemographic exploration of the milarite-type structure, Can. Mineral., 54, 1229–1247, https://doi.org/10.3749/canmin.1500088, 2016a.

Gagné, O. C. and Hawthorne, F. C.: Bond-length distributions for ions bonded to oxygen: alkali and alkaline-earth metals, Acta Crystallogr. B, B72, 602–625, https://doi.org/10.1107/S2052520616008507, 2016b.

Hawthorne, F. C., Kimata, M., Černý, P., Ball, N., Rossman, G. R., and Grice, J. D.: The crystal chemistry of the milarite-group minerals, Am. Mineral., 76, 1836–1856, 1991.

Hawthorne, F. C., Ungaretti, L., and Oberti, R.: Site populations in minerals; terminology and presentation of results of crystal-structure refinement, Can. Mineral., 33, 907–911, 1995.

Holder, R. M., Hacker, B. R., Horton, F., and Rakotondrazafy, A. F. M.: Ultrahigh-temperature osumilite gneisses in southern Madagascar record combined heat advection and high rates of radiogenic heat production in a long-lived high-T orogen, J. Metamorph. Geol., 36, 855–880, https://doi.org/10.1111/jmg.12316, 2018.

Klingelhöfer, G., Fegley Jr., B., Morris, R. V., Kankeleit, E., Held, P., Elvanov, E., and Priloutskii, O.: Mineralogical analysis of Martian soil and rock by a miniaturized backscattering Mössbauer spectrometer, Planet Space Sci., 44, 1277–1288, 1996.

Kröner, A., Hegner, E., Collins, A. S., Windley, B. F., Brewer, T. S., Razakamanana, T., and Pidgeon, R. T.: Age and magmatic history of the Antananarivo Block, central Madagascar as derived from zircon geochronology and Nd isotopic systematics, Am. J. Sci., 300, 251–288, 2000.

Lacroix, A.: Note préliminaire sur une nouvelle espèce minérale, B. Soc. Fra. Mineral., 25, 85–86, 1902.

Lacroix, A.: Sur une nouvelle espèce minérale (bityite) et sur les minéraux qu'elle accompagne dans les gisements tourmalinifères de Madagascar, Cr. Acad. Sci. Nat., 146, 1367–1371, 1908.

Lacroix, A.: Sur une nouvelle espèce minérale (manandonite) des pegmatites de Madagascar, B. Soc. Fra. Mineral., 35, 223–226, 1912.

Lafuente, B., Downs, R. T., Yang, H., and Stone, N.: The power of databases: the RRUFF project, in: Highlights in Mineralogical Crystallography, edited by: Armbruster, T. and Danisi, R. M., Walter de Gruyter GmbH, Berlin, Germany, 1–30, https://doi.org/10.1515/9783110417104, 2015.

Laurs, B. M., Simmons, W. B., Rossman, G. R., Quinn, E. P., McClure, S. F., Peretti, A., Armbruster, T., Hawthorne, F. C., Falster, A. U., Günther, D., Cooper, M. A., and Grobéty, B.: Pezzottaite from Ambatovita, Madagascar: A New Gem Mineral, Gems Gemol., 39, 284–301, 2003.

Lefevre, T. L. and Thomas, L.: Les pegmatites de la vallée de la Sahatany, Madagascar, Le Règne Minéral, 19, 15–28, 1998.

Lengauer, C. L., Hrauda, N., Kolitsch, U., Krickl, R., and Tillmanns, E.: Friedrichbeckeite, $K_{(0.5}Na_{0.5)2}(Mg_{0.8}Mn_{0.1}Fe_{0.1})_2(Be_{0.6}Mg_{0.4})_3[Si_{12}O_{30}]$, a new milarite-type mineral from the Bellerberg volcano, Eifel area, Germany, Miner. Petrol., 96, 221–232, https://doi.org/10.1007/s00710-009-0050-9, 2009.

Mandarino, J. A.: The Gladstone-Dale relationship. IV. The compatibility concept and its application, Can. Mineral., 41, 989–1002, 1981.

Mindat: Mineral species of Madagascar, available at: https://www.mindat.org/loc-2247.html, last access: 24 March 2020a.

Mindat: Sc-rich mineral species, available at: https://www.mindat.org/chemsearch.php?inc=Sc2Cexc=class=0sub=Search+Minerals, last access: 25 March 2020b.

Momma, K. and Izumi, F.: VESTA 3 for three-dimensional visualization of crystal, volumetric and morphology data, J. Appl. Crystallogr., 44, 1272–1276, https://doi.org/10.1107/S0021889811038970, 2011.

Nagashima, M., Fukuda, C., Matsumoto, T., Imaoka, T., Odicino, G., and Armellino, G.: Aluminosugilite, $KNa_2Al_2Li_3Si_{12}O_{30}$, an Al analogue of sugilite, from the Cerchiara mine, Liguria, Italy, Eur. J. Mineral., 32, 57–66, https://doi.org/10.5194/ejm-32-57-2020, 2020.

Pezzotta, F.: La pegmatite di Ambatovita, un giacimento ricco di micro-minerali, Rivista Mineralogica Italiana, 30, 100–101, 2005.

Robinson, K., Gibbs, G. V., and Ribbe, P. H.: Quadratic elongation: a quantitative measure of distortion in coordination polyhedra, Science, 172, 567–570, 1971.

Rossi, G., Smith, D. C., Ungaretti, L., and Domeneghetti, M. C.: Crystal-chemistry and cation ordering in the system diopside-jadeite: A detailed study by crystal structure refinement, Contrib. Mineral. Petrol., 83, 247–258, 1983.

Shannon, R. D.: Revised effective ionic radii and systematic studies of interatomic distances in halides and chalcogenides, Acta Crystallogr. A, 32, 751–767, 1976.

Sheldrick, G. M.: Crystal Structure refinement with SHELX, Acta Crystallogr. C, 71, 3–8, https://doi.org/10.1107/S2053229614024218, 2015.

Simmons, W. B., Pezzotta, F., Falster, A. U., and Webber, K. L.: Londonite, a new mineral species: the Cs-dominant analogue of rhodizite from the Antandrokomby granitic pegmatite, Madagascar, Can. Mineral., 39, 747–755, 2001.

Steffenssen, G., Müller, A., Rosing-Schow, N., and Friis, H.: The distribution and enrichment of scandium in garnets from the Tørdal pegmatites, south Norway, and its economic implications, Can. Mineral., 57, 799–801, https://doi.org/10.3749/canmin.AB00025, 2019.

Strunz, H. and Nickel, E. H.: Strunz mineralogical tables. Schweizerbart, Stuttgart, 869 pp., 2001.

Tucker, R. D., Ashwal, L. D., Handke, M. J., Hamilton, M. A., Le Grange, M., and Rambeloson, R. A.: U-Pb geochronology and isotope geochemistry of the Archean and Proterozoic rocks of north-central Madagascar, J. Geol., 107, 135–153, 1999.